AD-A172 295 PHOTOLUMINESCENT PROPERTIES OF N-GAAS ELECTRODES: SIMULTANEOUS DETERMINTT (U) WISCONSIN UNIV-MADISON DEPT OF CHEMISTRY A A BURK ET AL 10 SEP 86 1/1

UNCLASSIFIED UWIS/DC/TR-86/2 N00014-85-K-0631 F/G 9/1 NL

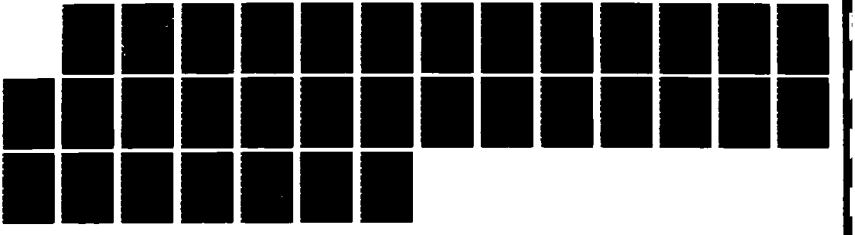

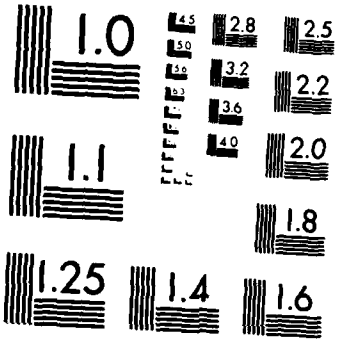

MICROCOPY RESOLUTION TEST CHART
NATIONAL BUREAU OF STANDARDS-1963-A

SECUR

AD-A172 295

RT DOCUMENTATION PAGE

1a. REPORT SECURITY CLASSIFICATION NA	1b. RESTRICTIVE MARKINGS NA
2a. SECURITY CLASSIFICATION AUTHORITY NA	3. DISTRIBUTION / AVAILABILITY OF REPORT Distribution Unlimited; Approved for Public Release
2b. DECLASSIFICATION / DOWNGRADING SCHEDULE NA	
4. PERFORMING ORGANIZATION REPORT NUMBER(S) UWIS/DC/TR-86/2	5. MONITORING ORGANIZATION REPORT NUMBER(S) NA
6a. NAME OF PERFORMING ORGANIZATION Chemistry Department University of Wisc.-Madison	6b. OFFICE SYMBOL (If applicable) NA
6c. ADDRESS (City, State, and ZIP Code) 1101 University Avenue Madison, WI 53706	7a. NAME OF MONITORING ORGANIZATION ONR
	7b. ADDRESS (City, State, and ZIP Code) 800 N. Quincy Street Arlington, VA 22217
8a. NAME OF FUNDING / SPONSORING ORGANIZATION	8b. OFFICE SYMBOL (If applicable) NA
	9. PROCUREMENT INSTRUMENT IDENTIFICATION NUMBER Contract N00014-85-K-0631
8c. ADDRESS (City, State, and ZIP Code)	10. SOURCE OF FUNDING NUMBERS

PROGRAM ELEMENT NO.	PROJECT NO.	TASK NO. R&T Code	WORK UNIT ACCESSION NO.
		4134003	

DTIC ELECTE SEP 25 1986 S E

11. TITLE (Include Security Classification)
Photoluminescent Properties of n-GaAs Electrodes: Simultaneous Determination of Depletion Widths and Surface Hole-Capture Velocities in Photoelectrochemical Cells

12. PERSONAL AUTHOR(S)
A.A. Burk, Jr., Phelps B. Johnson, William S. Hobson, and Arthur B. Ellis

13a. TYPE OF REPORT	13b. TIME COVERED	14. DATE OF REPORT (Year, Month, Day)	15. PAGE COUNT
Technical	FROM _____ TO _____	10/18/85	32

16. SUPPLEMENTARY NOTATION
Prepared for publication in the Journal of Applied Physics

17 COSATI CODES			18. SUBJECT TERMS (Continue on reverse if necessary and identify by block number)
FIELD	GROUP	SUB-GROUP	n-GaAs; photoluminescence; dead-layer model; depletion width; surface hole-capture velocity; photoelectrochemical cells

19. ABSTRACT (Continue on reverse if necessary and identify by block number)

Steady-state photoluminescence measurements performed on n-GaAs electrodes used in photoelectrochemical cells (PEC's) employing a stabilizing, aqueous telluride electrolyte yield values for the electrode's depletion width W and surface hole-capture velocity S. Between -1.0 V (a potential near short circuit) and -1.5 V vs. an SCE reference electrode (a potential near open circuit at the photon flux of 1×10^{15} photons/s/cm^2 employed), the interface behaves ideally: virtually all of the applied potential appears in the semiconductor space-charge region. Over this potential regime S is determined to be constant to within 10% and has a value, using literature values for hole lifetime and diffusion length, of approximately 2×10^5 cm/s for n-GaAs electrodes having carrier concentrations of $(1 - 4) \times 10^{17}$/cm^{-3}. Similar values of S obtained in air and in the PEC suggest a common rate-limiting mechanism for hole consumption in the two media.

20. DISTRIBUTION / AVAILABILITY OF ABSTRACT	21. ABSTRACT SECURITY CLASSIFICATION
☒ UNCLASSIFIED/UNLIMITED ☐ SAME AS RPT ☐ DTIC USERS	
22a. NAME OF RESPONSIBLE INDIVIDUAL Arthur B. Ellis	22b. TELEPHONE (Include Area Code) (608) 262-0421
	22c. OFFICE SYMBOL

DD FORM 1473, 84 MAR — 83 APR edition may be used until exhausted. All other editions are obsolete.

SECURITY CLASSIFICATION OF THIS PAGE
Unclassified

DTIC FILE COPY

OFFICE OF NAVAL RESEARCH

Contract N00014-85-K-0631

R&T Code 4134003

Technical Report No. UWIS/DC/TR-86/2

Photoluminescent Properties of n-GaAs Electrodes: Simultaneous Determination of Depletion Widths and Surface Hole-Capture Velocities in Photoelectrochemical Cells

by

A.A. Burk, Jr., Phelps B. Johnson, William S. Hobson, and Arthur B. Ellis*

Prepared for Publication in

Journal of Applied Physics

University of Wisconsin
Department of Chemistry
Madison, Wisconsin 53706

September 10, 1986

Accession For
NTIS GRA&I
DTIC TAB
Unannounced
Justification
By
Distribution/
Availability Codes
Dist | Avail and/or Special
A-1

QUALITY INSPECTED 1

Reproduction in whole or in part is permitted for any purpose of the United States Government

This document has been approved for public release and sale; its distribution is unlimited.

*To whom all correspondence should be addressed

86 9 25 04

Photoluminescent Properties of n-GaAs Electrodes: Simultaneous Determination of Depletion Widths and Surface Hole-Capture Velocities in Photoelectrochemical Cells

The study of photoelectrochemical cells (PEC's)[1] has prompted the development of in situ techniques for characterizing the semiconductor-electrolyte interface. A key question is the manner in which applied potential is partitioned across the semiconductor-liquid interface and the extent to which this depends on electrode surface properties. Of particular value, then, are probes for the semiconductor electrode of its depletion width and surface recombination velocity, more aptly described for an electrode as a surface capture velocity (vide infra). The depletion width W has typically been estimated from capacitance data. The surface capture velocity S has been determined for very few semiconductor electrodes. Available values were obtained from temporal photoluminescence (PL) data on CdS[2] electrodes and surface photovoltage measurements on CdSe[3] electrodes. Ideally, one desires measurements of W and S under the steady-state conditions typically employed in PEC operation. The ability to readily evaluate these parameters can be expected to have a major impact in assessing the effects of electrolytes, etchants, and various electrode coatings

(metals, conductive polymers, derivatized surfaces, etc.) on electrode performance. Moreover, knowledge of W and S for semiconductor electrodes provides a direct link for comparing these solid-liquid interfaces to other semiconductor-derived interfaces involving gases, metals, and other semiconductors.

We have used steady-state PL measurements to determine the widths of electric fields in a variety of homogeneous[4] electrodes and inhomogeneous electrodes containing graded regions[5], isotype heterojunctions[6], and strained-layer superlattices.[7] For homogeneous electrodes, a simple dead-layer model was employed to estimate the depletion width from PL quenching data: The model assumes that electron-hole pairs formed within a distance on the order of the depletion width do not radiatively recombine.[8] While our PL data for n-GaAs electrodes were in good accord with this model, the treatment does not permit the evaluation of S and yields only changes in depletion width. A more sophisticated model, permitting the simultaneous determination of W and S from measurements of PL intensity as a function of optical penetration depth, was reported by Mettler and applied to n- and p-GaAs samples in air.[9] The generalization of this work to the semiconductor-electrolyte interface was originally outlined by Hobson.[10]

In this paper, we report the results of this extension of Mettler's treatment to an n-GaAs-based PEC employing a stabilizing aqueous telluride electrolyte. By determining S and W for n-GaAs electrodes spanning a range of carrier concentrations, we demonstrate that S is large and relatively insensitive to applied potential. Additionally, virtually all of the applied potential appears in the semiconductor over potentials between short circuit and the open-circuit voltage, the region corresponding to optical-to-electrical energy conversion. Moreover, PL data obtained in air yield values of S which are comparable to those obtained in the PEC, suggesting a common rate-limiting mechanism for hole consumption in these two media.

THEORY

The quantitative form of the dead-layer model (DLM) is given by Eq. (1), where ϕ_1 and ϕ_2 are the radiative efficiencies at two arbitrary potentials wherein the semiconductor is in depletion; $\alpha' = (\alpha_e + \alpha_p)$, where α_e and α_p, are the solid's absorptivities for the exciting and emitted light, respectively; and ΔD is the change in dead-layer thickness. If one of the potentials is the flat-band potential V_{FB}, then the PL intensity ratio yields the absolute dead-layer thickness D, assumed to be

roughly equal to W.

$$\frac{\phi_1}{\phi_2} = \exp(-\alpha'\Delta D) \qquad (1)$$

Calculation of D or ΔD simply requires measurement of the PL quenching between the potentials of interest and knowledge of the solid's absorptivities. Note that this treatment neglects S.

Our treatment closely follows the formalism derived by Mettler.[9] His treatment retains the dead-layer concept but also considers the effects on PL intensity of minority carrier diffusion to the dead layer and the nonradiative loss of these carriers at the semiconductor surface. Equation (2) describes the dependence of the normalized PL intensity I_L on the semiconductor's bulk and surface properties. I_L is the observed PL intensity divided by the excitation intensity, corrected for reflective losses. In this equation,

$$I_L = K\exp[-(\alpha_e + \alpha_p)W]\frac{\alpha_e L_p}{(\alpha_e L_p)^2 - 1} \times \left[\frac{S_r + \alpha_e L_p}{(S_r + 1)(\alpha_p L_p + 1)} - \frac{1}{(\alpha_e + \alpha_p)L_p}\right] \qquad (2)$$

K is a constant containing the internal quantum efficiency and geometric factors; L_p is the hole diffusion length; and S_r is the reduced surface hole-capture velocity. Values of S_r are related to the surface hole-capture velocity S by Eq. (3), where τ_p is the hole lifetime. Our use of the term "surface hole-capture velocity", rather than the conventional term "surface recombination velocity" used in Mettler's paper, encompasses both surface recombination and interfacial charge-transfer processes as sources of hole consumption. Whichever term is used, Mettler has pointed out that this parameter represents the rate at which holes pass from the neutral zone of the semiconductor into the depletion region.

$$S_r = \frac{S\tau_p}{L_p} \qquad (3)$$

The derivation of Equation (2) assumes that the optical penetration depth (OPD) is less than the hole diffusion length, i.e., $\alpha_e^{-1} < L_p$. A plot of I_L vs. α_e^{-1} can be fit to Equation (2) to yield values of W and S_r. Such I_L-OPD plots can be made at various applied potentials in a common geometry in a PEC. From Equation (2), the ratio of PL intensities at two potentials, V_1 and

V_2, leads to Equation (4). This ratio, Q, describes the manner in which the quenching of PL intensity depends on excitation wavelength and semiconductor properties.

$$Q = \frac{I_L(V_1)}{I_L(V_2)} = \exp\left[-(\alpha_e + \alpha_p)(W(V_1) - W(V_2))\right] \times \frac{[\ ]_{V_1}}{[\ ]_{V_2}} \qquad (4)$$

$$\text{where } [\ ]_V = \frac{S_r(V) + \alpha_e L_p}{(S_r(V) + 1)(\alpha_p L_p + 1)} - \frac{1}{(\alpha_e + \alpha_p)L_p}$$

It is noteworthy that Equation (4) reduces to Equation (1), if S_r is either relatively large ($S_r >> L_p/\tau_p$ and $\alpha_e L_p^2/\tau_p$) or independent of the applied potential.[4]

In practice, we obtain W and S_r at the open-circuit voltage (OCV) by fitting the I_L-OPD curve to Equation (2). Although W and S_r values could be obtained in the same way from data acquired at in-circuit potentials, considerably smaller standard deviations result from fitting Q-OPD curves to Eq. (4), forming the ratio with the open-circuit data. The improved relative values result from cancellation of systematic errors in the ratio. From W, we also obtained the Schottky barrier height V_B using Equation (5), where ε is the semiconductor's dielectric

constant (taken as 12.9[11]),

$$W = (2 \varepsilon \varepsilon_o V_B/q N_D)^{1/2} \quad (5)$$

ε_o is the permittivity of vacuum; q is the electronic charge; and N_D is the donor concentration. This equation allows determination of V_{FB}, since the two are related by Eq. (6).

$$V_B = V - V_{FB} \quad (6)$$

Equations (5), (6), and (1) can be combined to yield Eq. (7), which predicts the PL intensity as a function of electrode potential (LV curves), assuming large or relatively constant S_r and ideal behavior, i.e., all of the applied potential appears in the semiconductor electrode.

$$I_L = I_{L(FB)} \exp[-\alpha'(2\varepsilon \varepsilon_o(V-V_{FB})/q N_D)^{1/2}] \quad (7)$$

The LV curves can be fit to Eq. (7) (where $I_{L(FB)}$ is the PL intensity at flatband) and extrapolated to provide another estimate of the flat-band potential, subject to the aforementioned assumptions.

Reliable absorptivities and hole diffusion lengths are necessary for the acquisition and analysis of I_L-OPD and Q-OPD curves. Values of α_e based on transmission measurements were used between 600 and 750 nm.[12] Absorptivities at shorter wavelengths were obtained using Equation (1): a constant value for ΔD should be obtained irrespective of excitation wavelength, so that if α_e is known at one wavelength, values at other wavelengths can be readily determined from PL measurements. We found excellent consistency in ΔD using the absorptivities reported for 600 to 750 nm, and extended the values from PL quenching data to 400 nm, as shown in Figure 1. As an independent check, our absorptivities in the short wavelength regime are in good accord with the approximate Kramers-Kronig values.[13] The self-consistent absorptivities of Figure 1 were employed in all subsequent calculations. Hole diffusion lengths also appear in Eqs. (2) and (4). A literature value of 2 μm was used for all carrier concentrations.[14,15]

EXPERIMENTAL

All samples of n-GaAs were oriented perpendicular to the (100) face and were Te doped; the sources and physical properties of the samples are given in Table II. Crystals (approximately 5 x 5 x 0.1 mm^3) were mounted as described elsewhere[16] and etched before use to a mirrored surface in a 5:1:1 H_2SO_4:H_2O_2:H_2O solution at 295 K. Telluride electrolyte, synthesized as previously described[17], typically had a composition of 7.5 M KOH/0.2 M Te^{2-}/<0.006 M Te_2^{2-} (redox potential of approximately -1.18 V vs. SCE). Potentiostatic experiments were conducted with a standard three-electrode setup using cells and electrochemical equipment previously described.[16]

The experimental apparatus is shown in Figure 2. An Oriel Model 7292 150-W Xe lamp was used with assorted colored glass, bandpass, interference and neutral density filters to provide a variable excitation wavelength source with approximately 10 nm bandwidth. A lens was used to approximately collimate the light to a homogeneous beam having the dimensions of the crystal surface. A BK-7 glass neutral-density filter was calibrated as a beam splitter for monitoring excitation intensity, which was approximately photon-matched with neutral density filters, as determined by a calibrated EG&G Model 550-1 radiometer.

Front-surface PL was monitored in air and during PEC operation. All of the GaAs samples exhibited PL with

uncorrected λ_{max} values of ~864 nm (1.43 eV), corresponding to the band gap energy.[18] Between open circuit and potentials slightly positive of short circuit, no change in the PL spectral distribution was seen at low resolution (2 nm), permitting changes in PL to be monitored at a single wavelength, λ_{max}. Front-surface PL was measured using photon-counting techniques. The experimental setup consisted of a cooled GaAs PMT, a 0.35-m McPherson monochromator, and a LeCroy Model 4604 photon counter. Both the lamp and photon counter outputs were monitored with an Apple IIe microcomputer; corrections were made for detector response, reflective losses[13] and the beam splitter's calibration curve. An intensity of roughly 1 x 10^{15} photons/s-cm^2 (~0.5 mW/cm^2 at 460 nm) was used in obtaining I_L-OPD plots. Absorptivities were obtained as described in the text from PL quenching data. In these experiments, PL quenching was monitored between open circuit and -1.0 V vs. SCE for wavelengths between 400 and 750 nm. The absorptivities acquired for n-GaAs samples with carrier concentrations of 1.5 x 10^{17} cm^{-3} and 5 x 10^{17} cm^{-3} were virtually identical. The generated I_L-OPD (Eq. (2)) and Q-OPD (Eq. (4)) curves were fit using a nonlinear least squares curve fitting program. In addition, conventional luminescence-voltage curves, LV's, were taken using several laser

lines, provided by Coherent Radiation Model CR-12 Ar^+ and Innova K3000 Kr^+ lasers, and fit to Eq. (7). Capacitance measurements for constructing Mott-Schottky plots were made at 950 Hz with an Ithaco Model 391 lock-in voltmeter and PAR Model 173 potentiostat and Model 175 programmer.

RESULTS

PL Properties in a PEC

Typical plots of PL intensity and photocurrent vs. applied potential for a n-GaAs-based PEC employing telluride electrolyte are shown in Figure 3. At potentials anodic of the OCV, PL quenching is consistent with simple dead-layer behavior. Data from Q-OPD curves and LV curves demonstrate that virtually all applied potential appears in the semiconductor between -1.0 and -1.5 V (approximately the OCV) vs. SCE, the potential regime corresponding to optical-to-electrical energy conversion.

Representative I_L-OPD plots obtained for an n-GaAs electrode at the OCV and a potential near short circuit (-1.0 V vs. SCE) are shown in Figure 4. Values of S_r and W extracted at these and several other potentials are shown in Table I. These data indicate that S_r is constant to within 10% between -1.0 V vs. SCE and the OCV. The value for S_r of approximately 15 corresponds to a surface hole-

capture velocity of approximately 2×10^5 cm/s, using literature values of 20 ns for τ_p[14] and 2 μm for L_p[14] (Eq. (3)). The large and relatively potential-independent value of S_r justifies the use of the simple dead-layer model (Eq.(1)) for this PEC.[4,10]

In contrast to S_r, W increases substantially for potentials anodic of the OCV, in good accord with the simple dead-layer model. It is noteworthy that a substantial electric field exists in the electrode at the OCV: a value for W of 850 Å, corresponding to a barrier height of approximately 730 mV, was obtained. Our data indicate that the PEC behaves ideally at potentials anodic of the OCV. The values of V_B determined from the Q-OPD curves are in excellent agreement with the sum of the barrier height at the OCV and the difference in electrode potential from the OCV, as shown in Table I, indicating that almost all of the applied potential appears in the semiconductor electrode.

Another illustration of the ideality of this PEC is provided by Figure 5, which compares the experimental PL intensity curve obtained with 457.9-nm excitation to that predicted using Eq. (7), which assumes ideal behavior. The flat-band potential used in this calculation is -2.23 V vs. SCE, obtained from the data of Table I. This value for V_{FB} is consistent with an estimate of -2.2 V from dark

capacitance data. It also accords well with a dark value of -2.1 V reported for a selenide electrolyte from capacitance measurements; in that study, an anodic shift of V_{FB} to -1.7 V vs. SCE at an excitation intensity of 20 mW/cm^2 was reported.[19,20] Our photon flux, $\sim$40 times weaker, does not substantially shift V_{FB} relative to the dark value.

The aforementioned results are illustrative of those obtained for a variety of n-GaAs electrodes with carrier concentrations ranging from approximately 5 x 10^{16} to 1 x 10^{18} cm^{-3}. All of these electrodes behave ideally at potentials anodic of the OCV, and their surface hole-capture velocities are constant to within 10% out to -1.0 V vs. SCE. Table II summarizes the values of W and S_r at the OCV of each electrode, approximately -1.5 V vs. SCE. The table indicates that Schottky barriers of roughly 650 to 900 mV are observed at this potential. Values of S_r tend to fall between 10 and 25 for all but the extremes in carrier concentrations. However, the latter values are considerably more uncertain for two different experimental reasons: At the lowest carrier concentration employed (4.9 x 10^{16} cm^{-3}), the PL intensity was extremely weak; at the highest carrier concentration (9.6 x 10^{17} cm^{-3}) there is minimal band bending, resulting in greater relative uncertainty in W and in S_r.

Comparisons with PL Properties in Air and Mechanistic Implications

A compilation of W and S_r values obtained for these same n-GaAs samples in air from I_L-OPD plots are given in Table II. There is a striking similarity in S_r and W for each sample in these drastically different environments. The value of V_B obtained in air is in reasonable agreement with that observed by Mettler[9] and is consistent with values for n-GaAs-metal Schottky barriers.[21]

The similarity of S_r values in air and in the telluride electrolyte is intriguing from a mechanistic standpoint. With the n-GaAs-air interface, holes recombine with electrons via surface states within the bandgap; direct nonradiative recombination between the conduction and valence bands is extremely unlikely.[22] In contrast, holes photogenerated in an n-GaAs electrode immersed in telluride electrolyte can be captured either by electrons in the solid or by the solution reductant. At potentials where the photocurrent quantum yield approaches unity, the latter pathway dominates; at potentials characterized by lower quantum yields, additional information is needed to assess the contributions of the two hole-consumption routes, since hole capture by the electrolyte may or may not lead to Faradaic current. The nearly identical rates observed for

these two paths suggest a common rate-limiting step for hole consumption. Assuming that the literature values used to calculate S from S_r are good estimates for our samples, quantities in the range of 2×10^5 cm/s indicate that the supply of holes to the depletion region is not the common rate-limiting step: the thermal velocity of holes in n-GaAs is at least an order of magnitude larger than our values of S.[23] The more likely explanation, we believe, is that hole capture by surface states is rate-limiting in both air and in the PEC. This suggests that charge transfer is mediated by surface states in n-GaAs, in agreement with the conclusion reached by Allongue and Cachet.[24]

CONCLUSION

We have demonstrated that PL can be used to monitor the depletion width W and surface hole-capture velocity S_r of n-GaAs while the semiconductor serves as the photoanode in an operating PEC. These techniques, which permit determination of the manner in which applied potential is partitioned across the semiconductor-electrolyte interface, reveal this interface to behave ideally in the potential regime corresponding to optical-to-electrical energy conversion. The similarity of S_r in air and in telluride electrolyte suggests that holes are consumed in both cases by a common rate-limiting step, perhaps

involving transfer to intrabandgap surface states. Work is being expanded to include studies of surface modification and excitation intensity effects on GaAs and other semiconductors in PEC's.

ACKNOWLEDGMENTS

We wish to express our gratitude for experimental assistance to Mr. Chris McMillan and for assistance with computer programming to Mr. Hal Van Ryswyk. We thank Mr. Alan Huelsman for determining carrier concentrations. Dr. Shimshon Gottesfeld, Dr. Dennis Evans and Dr. John D. Wiley are thanked for helpful discussions. The authors thank the Office of Naval Research and the Army Research Office for support of this research. Phelps B. Johnson gratefully acknowledges support as a 1985 Electrochemical Society Summer Energy Research Fellow.

References

1. M. S. Wrighton, Acc. Chem. Res. 12, 303 (1979); A. J. Bard, Science 207, 139 (1980); A. Heller, Acc. Chem. Res. 14, 154 (1981).

2. M. Evenor, S. Gottesfeld, Z. Harzion, D. Huppert, and S. W. Feldberg, J. Phys. Chem. 88, 6213 (1984).

3. G. J. Storr and D. Haneman, J. Appl. Phys. 58, 1667 (1985).

4. W. S. Hobson and A. B. Ellis, J. Appl. Phys. 54, 5956 (1983).

5. M. K. Carpenter and A. B. Ellis, J. Electroanal. Chem 184, 289 (1985).

6. W. S. Hobson, P. B. Johnson, A. B. Ellis, and R. M. Biefeld, Appl. Phys. Lett. 45, 150 (1984).

7. P. B. Johnson, A. B. Ellis, R. M. Biefeld, and D. S. Ginley, Appl. Phys. Lett. 47, 877 (1985)

8. R. E. Hollingsworth and J. R. Sites, J. Appl. Phys. 53, 5357 (1982) and references therein.

9. K. Mettler, Appl. Phys. 12, 75 (1977).

10. W. S. Hobson, Ph.D. Thesis, University of Wisconsin (1984).

11. G. E. Stillman, C. M. Wolfe, and J. O. Dimmock, in Semiconductors and Semimetals, edited by R. K. Willardson and A. C. Beer (Academic, New York, 1977) Vol. 12, p. 169.

12. M. D. Sturge, Phys. Rev. 127, 768 (1962).

13. B. O. Seraphin and H. E. Bennett in Semiconductors and Semimetals, edited by R. K. Willardson and A. C. Beer (Academic, New York, 1967) Vol. 3, p. 499

14. C. J. Hwang, J. Appl. Phys. 54, 4408 (1971).

15. The surface parameters W and S_r were relatively insensitive to modest changes in the bulk parameters L_p and α_p: for example, changes in L_p of ±25% typically led to changes in W and S_r of ±2% and 10%, respectively; changes in α_p of ±25% produce variations in W and S_r of ∓3% and ±20%, respectively. We were unable to fit I_L-OPD curves to Eq. (2) when $L_p \lesssim 1\mu m$, while satisfactory fits can still be obtained for arbitrarily large values of L_p. As expected, W and S_r were more sensitive to variations in α_e^{-1}: If α_e^{-1} values are increased by 25 % at all wavelengths, W and S_r increase by 15% and 30%, respectively; if α_e^{-1} values are decreased by 25%, W and S_r decrease by 20% and 10%, respectively.

16. B. R. Karas and A. B. Ellis, J. Am. Chem. Soc. 102, 968 (1980).

17. W. S. Hobson and A. B. Ellis, Appl. Phys. Lett. 41, 891 (1982).

18. D. D. Sell and H. C. Casey, Jr., J. Appl. Phys. 45, 800 (1974).

19. G. Horowitz, P. Allongue and H. Cachet, J.

Electrochem. Soc. 131, 2563 (1984).

20. P. Allongue, H. Cachet, and G. Horowitz, J. Electrochem. Soc. 130, 2352 (1983).

21. S. M. Sze in Physics of Semiconductor Devices, (John Wiley, New York, 1981) p. 291.

22. J. S. Blakemore in Semiconductor Statistics (part of an International Series of Monographs on Semiconductors), edited by H. K. Henisch (Pergamon, New York, 1962) Vol. 3, p. 193.

23. D. E. Aspnes, Surface Science, 132, 406 (1983): we assumed a hole effective mass of 0.45 m_e, taken from reference 21 p. 850.

24. P. Allongue and H. Cachet, Solid State Commun. 55, 49 (1985).

Table I. Electrode Parameters of a n-GaAs-based PEC.[a]

Volts vs. SCE[b]	W, Å[c]	V_B, (mV)[d]	[V_B (at -1.50V) + ΔV], mV[e]	S_r[f]
-1.00	1080	1200	1230	15.8
-1.10	1040	1100	1130	15.6
-1.20	990	1000	1030	15.6
-1.28	950	930	950	15.2
-1.36	910	850	870	15.1
-1.44	860	760	790	15.0
-1.50	850	730	730	14.8

[a]Properties derived from PL of an n-GaAs electrode (no. 2, cf. Table II, footnote b) having n=1.5 x 10^{17} cm^{-3}. The PEC consisted of a three-electrode potentiostatic setup and telluride electrolyte. Table entries are extracted from I_L-OPD curves like those shown in Figure 4 and Q-OPD curves. Vigorous magnetic stirring and a N_2 blanket were used in all PEC experiments. The influence of uncertainties in bulk parameters on the table entries is discussed in footnote 15.

[b]Electrode potential of the n-GaAs electrode.

[c]Depletion width at the indicated potential, obtained by fitting Q-OPD curves to Eq. (4); at -1.50 V vs. SCE, W is obtained by fitting the I_L-OPD curve to Eq. (2). The absolute error in W from fitting the I_L-OPD curve at -1.5 V vs. SCE is

±10%; however, the relative error between values in the table obtained from Q-OPD curves is ±0.5%.

[d]Barrier height obtained from W using Eq. (5).

[e]Barrier height calculated assuming ideal electrode behavior. The indicated value is the sum of the barrier height at -1.50 V vs. SCE (730 mV) and the difference in electrode potential from -1.50 V vs. SCE.

[f]Reduced surface hole-capture velocity at the indicated potential, obtained by fitting Q-OPD curves to Eq. (4); at -1.50 V vs. SCE, S_r is obtained by fitting the I_L-OPD curve to Eq. (2). The absolute error in S_r from fitting the I_L-OPD curve at -1.5 V vs. SCE is ±25%; however, the relative error between values in the table obtained from Q-OPD curves is ±2.5%.

Table II. Comparison of Parameters for n-GaAs Samples in Air and in a PEC.[a]

Electrode no. ($n \times 10^{-16}$, cm^{-3})[b]	W, Å (Te_n^{2-})[c]	V_B (mV)[d]	S_r (Te_n^{2-})[e]	W, Å (air)[f]	S_r (air)[g]
1 (4.9)	1600	750	2	1600	8
2 (15)	810	670	15	800	17
3 (25)	660	780	16	640	14
4 (32)	600	810	10	590	8
5 (41)	470	640	23	450	27
6 (96)	380	900	35	350	38

[a]Properties derived from PL of n-GaAs samples. Table entries are extracted from I_L-OPD curves like those shown in Figure 4. The influence of uncertainties in bulk parameters on the table entries is discussed in footnote 15.

[b]Carrier concentrations of n-GaAs electrodes, as determined by Hall measurements, are given in parentheses. Electrodes 1, 2, 3, and 5 are melt-grown samples from Morgan Semiconductors, Inc. Electrodes 4 and 6 are melt-grown samples from Laser Diode, Inc. All electrodes are Te-doped except for no. 2 which is Si-doped.

[c]Depletion width at -1.5 V vs. SCE in telluride electrolyte (a potential at or near open circuit for all samples), obtained by fitting I_L-OPD curves to Eq. (2). The absolute error in W from

fitting the I_L-OPD curves is ±10%.

[d]Barrier height obtained from W using Eq. (5).

[e]Reduced surface hole-capture velocity at -1.5 V vs. SCE in telluride electrolyte, obtained by fitting I_L-OPD curves to Eq. (2). The absolute error in S_r from fitting the I_L-OPD curves is ± 25%.

[f]Depletion width in air, obtained by fitting I_L-OPD curves to Eq. (2). Errors associated with this measurement are contained in footnote c of this table.

[g]Reduced surface hole-capture velocities in air, obtained by fitting the I_L-OPD curves to Eq. (2). Errors associated with this measurement are contained in footnote e of this table.

Figure Captions

FIG. 1. Reciprocal absorptivities for GaAs, determined as described in the text.

FIG. 2. Apparatus for monitoring PL of a semiconductor electrode while operating in a PEC:
A. Xe lamp; B. Optical filters; C. Collimating lens; D. Beam splitter; E. Standard three-electrode PEC including semiconductor photoelectrode, Pt counterelectrode, saturated calomel reference electrode and telluride electrolyte; F. Potentiostat; G. Collection lens; H. Filter to remove exciting light; I. Monochromator; J. PMT; K. Photon counter; L. Microcomputer; M . Radiometer; N. Radiometer probe head.

FIG. 3. Relative photocurrent (bottom panel) and PL intensity (top panel) as a function of potential for an n-GaAs-based PEC employing telluride electrolyte; PL intensity was monitored at λ_{max}, 864 nm. Electrode no. 2 with n = 1.5 x 10^{17} cm^{-3} was excited with 0.5 mW/cm^2 of 457.9-nm light. Photocurrents are relative to the value at -1.0 V vs. SCE ($\sim$0.1 mA/cm^2). The above curves were swept simultaneously at 5 mV/s.

FIG. 4. Photoluminescence intensity vs. optical

penetration depth (I_L-OPD curves) for electrode no. 2 at two electrode potentials, -1.5 V vs. SCE (circles) and -1.0 V vs. SCE (squares). The solid lines are the best fits to Eq. (2). Values of S_r and W extracted at these potentials are given in Table I. An excitation intensity of $\sim 1 \times 10^{15}$ photons/s-cm^2 was used throughout the experiment.

FIG. 5. PL intensity as a function of applied potential for n-GaAs electrode no. 2 in a PEC employing telluride electrolyte. The squares are experimental data acquired with 457.9 nm-excitation. The solid line is the fit to Eq. (7), using a value for V_{FB} obtained from the I_L-OPD curves typified by those in Figure 4.

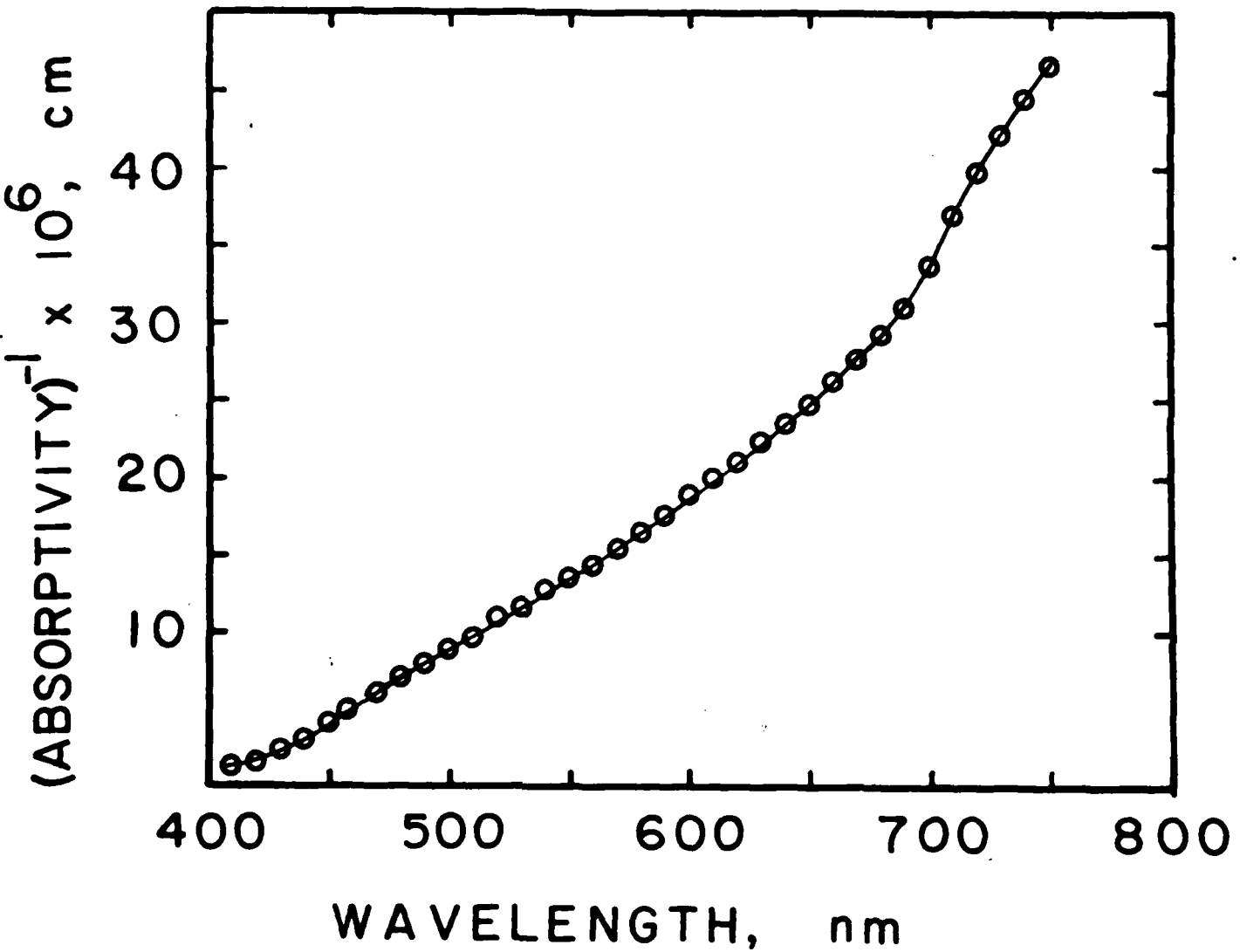
(ABSORPTIVITY)$^{-1}$ x 10^6, cm
40
30
20
10
400
500
600
700
800
WAVELENGTH, nm

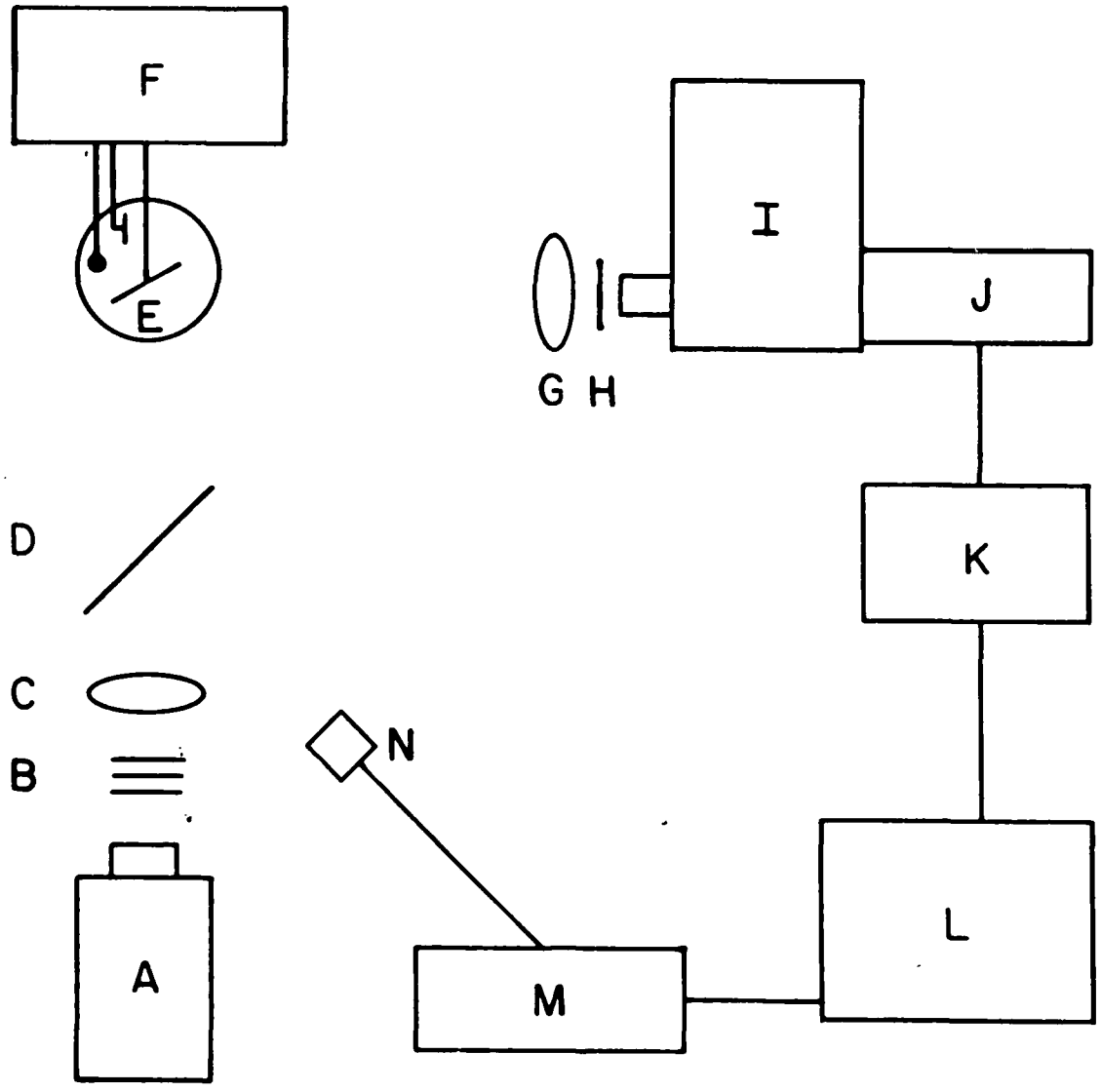
F
4
E
I
J
G H
K
D
C
B
N
A
M
L

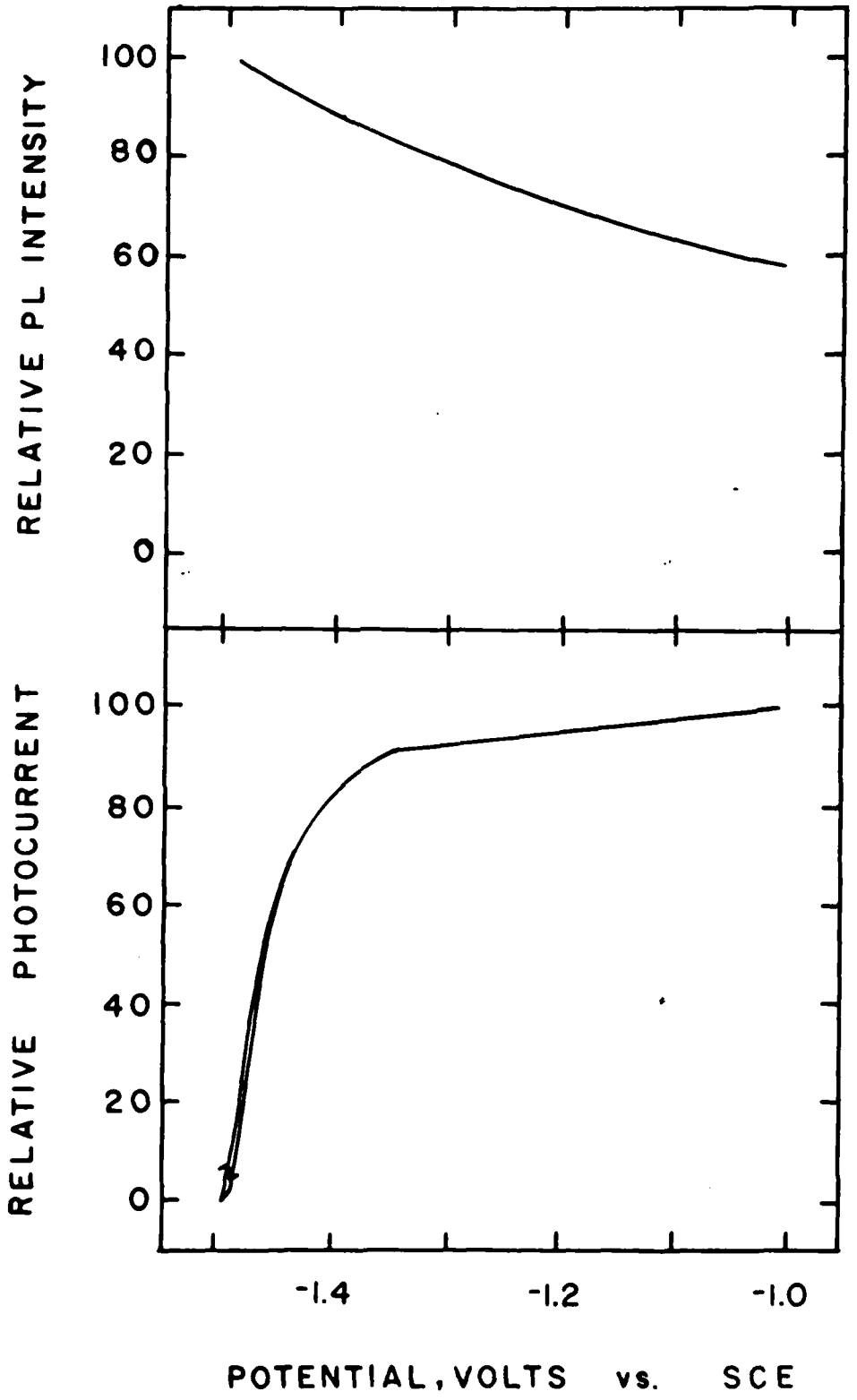
RELATIVE PL INTENSITY
100
80
60
40
20
0
RELATIVE PHOTOCURRENT
100
80
60
40
20
0
-1.4
-1.2
-1.0
POTENTIAL, VOLTS vs. SCE

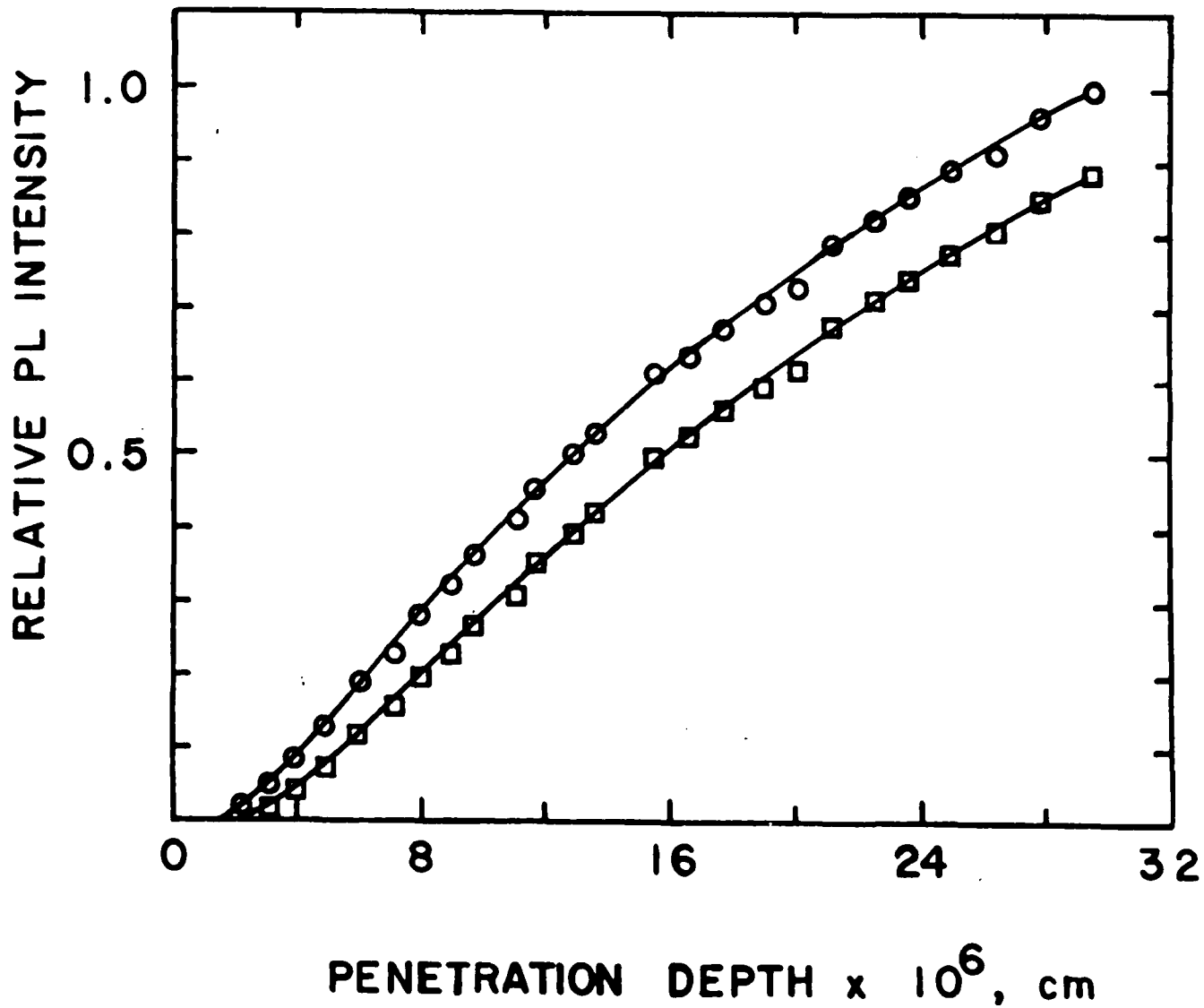
RELATIVE PL INTENSITY
1.0
0.5
0
8
16
24
32
PENETRATION DEPTH x 10^6, cm

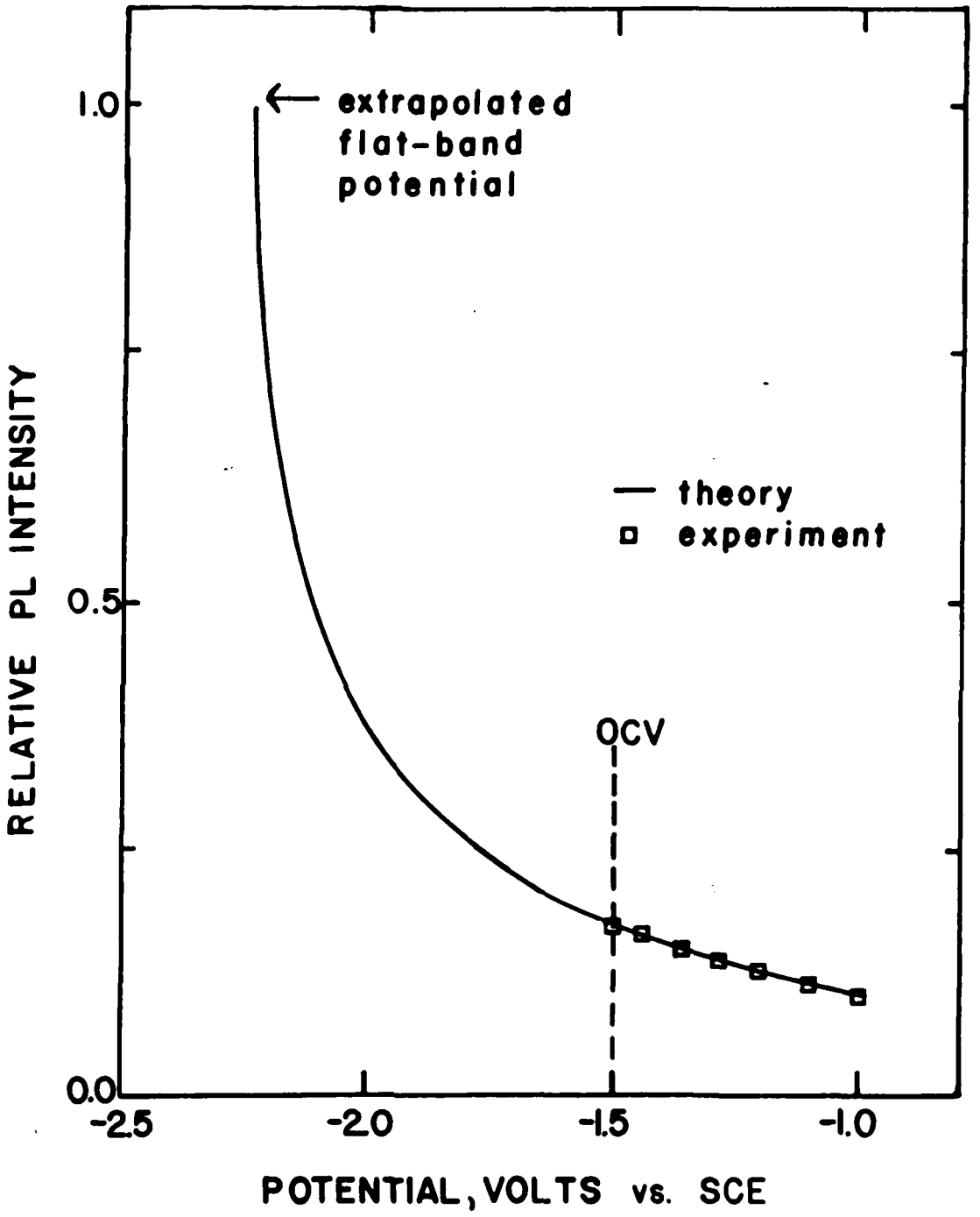
1.0
0.5
0.0
-2.5
-2.0
-1.5
-1.0
← extrapolated
flat-band
potential
— theory
□ experiment
OCV
RELATIVE PL INTENSITY
POTENTIAL, VOLTS vs. SCE

END

10-86

DTIC